Title	Process parameters and their effect on metal transfer in gas metal arc welding: a driving force perspective
Author(s)	Sato, Yuriko; Ogino, Yosuke; Sano, Tomokazu
Citation	Welding in the World. 2024, 68, p. 905-913
Version Type	VoR
URL	https://hdl.handle.net/11094/94638
rights	This article is licensed under a Creative Commons Attribution 4.0 International License.
Note	

RESEARCH PAPER

Process parameters and their effect on metal transfer in gas metal arc welding: a driving force perspective

Yuriko Sato[1] · Yosuke Ogino[1] · Tomokazu Sano[1]

Abstract

In gas metal arc welding (GMAW), the optimization of process parameters and the control of metal transfer is pivotal for achieving superior welding outcomes. This study meticulously examines the roles of core process parameters in metal transfer: wire extension and arc geometry, which includes arc length and inter-cathode distance. Using a unique MIG-based non-transferred arc system with symmetrically arranged tungsten cathodes we have achieved distinct control over wire feed rate and arc geometry, independent of the arc current. We investigate the interplay of these parameters and their consequential influence on the driving forces governing metal transfer. While increasing the wire extension enhanced inertial forces, it did not lead to consistent transitions in the metal transfer modes. In contrast, adjusting arc length and inter-cathode distance effectively controlled the electromagnetic force acting on molten droplets, as quantified by the arc spread angle θ. Notably, an increase in the arc spread angle resulted in the elongation of molten droplets. This study clarifies the fundamental relationships between driving forces and process parameters in GMAW. Additionally, it introduces a more advanced evaluation model for electromagnetic force and offers a comprehensive strategy for refining welding control techniques.

Keywords Gas metal arc welding · Metal transfer · Wire feed rate · Arc plasma geometry · Electromagnetic force · Inertial force

1 Introduction

Gas metal arc welding (GMAW) is a widely utilized welding method across various industries due to its high productivity and versatility. The quality and effectiveness of GMAW depend heavily on heat input and deposition rate, governed by two key process parameters: welding current and wire feed rate, respectively. Traditionally, these parameters are understood to be interdependent, with the wire feed rate typically increasing alongside the welding current [1]. Furthermore, these parameters are intricately connected to the 'driving forces' that govern the 'metal transfer' phenomenon in GMAW.

The metal transfer process, where molten metal is transferred from a welding wire to a workpiece, is a critical aspect of GMAW. The metal transfer process can occur in different modes, including short-circuit, globular, and spray transfer, the latter of which can exhibit variations such as projected-spray and streaming-spray transfer. Each mode is characterized by distinct features and is suitable for specific applications, and the dominant forces determining the metal transfer can vary with each [2].

In GMAW, the welding current primarily controls the electromagnetic force, a key driving force in the metal transfer process. The higher the welding current, the stronger the electromagnetic force, which in turn influences the formation and detachment of droplets at the electrode tip [3]. On the other hand, the wire feed rate is believed to impact the inertial forces during metal transfer. This has been insightfully likened to water dripping from an orifice by Lancaster [4]. In this analogy, the outflow speed, akin to the wire feed rate in GMAW, determines the magnitude of the inertial force.

Despite these insights, gaps exist in our understanding of how variations in these process parameters directly affect

these driving forces and ultimately, the metal transfer process. While the relationship between increased welding current and wire feed rate is commonly observed, this relationship is often accepted without detailed investigations into its effects on the driving forces involved in metal transfer. Furthermore, the effects of independently controlling these parameters remain largely unexplored.

This study aims to delve deeper into the effects of independently controlling welding current and wire feed rate on the metal transfer process in GMAW. By challenging the conventional understanding of the interdependence of these parameters, we aim to explore the potential for a more nuanced control. We seek to fill the identified knowledge gaps by providing a detailed analysis of how process parameters correlate with driving forces in different metal transfer modes. This investigation is expected to offer significant insights into the GMAW process and potentially facilitate improved control over welding quality.
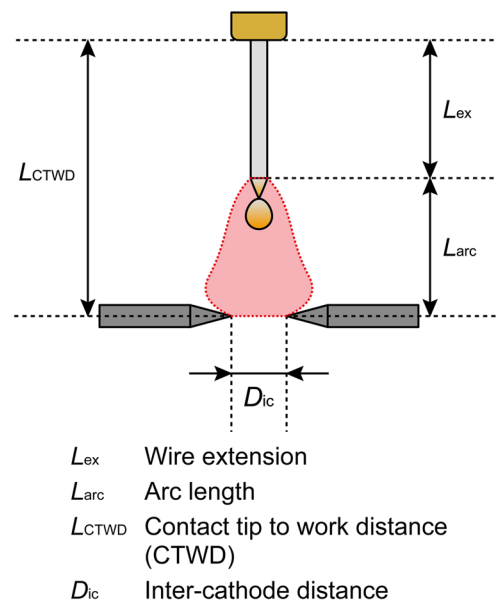
2 Experimental setup and methodology

In this study, we adopted a unique non-transferred arc system involving two tungsten cathodes, enabling the independent control of the wire feed rate and arc current. This setup represents a novel fusion of elements from metal inert gas (MIG) and tungsten inert gas (TIG) welding, with the primary aim of finely controlling the arc geometry. This goal contrasts with previous studies that have applied MIG-TIG hybrid system for different purposes. For instance, Ando et al. [5] designed such a setup to extract droplets from the arc plasma for calorimetric analysis, while Wang et al. aimed at minimizing the heat input into the workpiece [6, 7]. Conversely, our focus was on fine-tuning the arc geometry to achieve independent control over the arc current and wire feed rate.

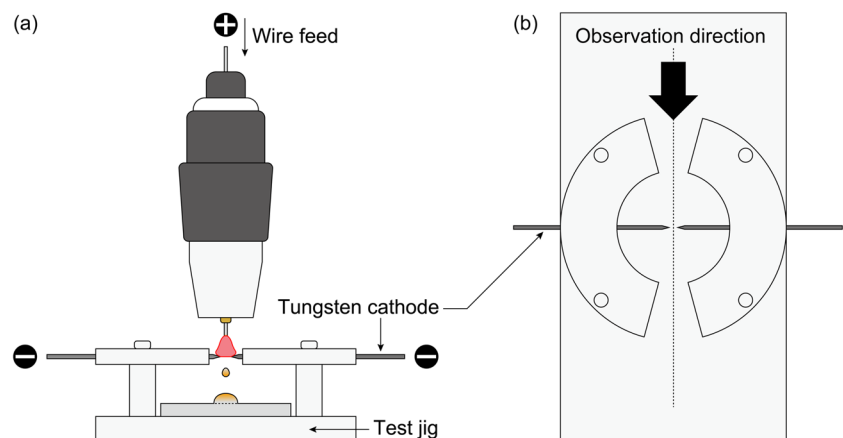The experimental setup, designed to ensure a symmetric arc geometry, was as follows (Fig. 1(a)): a constant current power source (Welbee Inverter T500P, DAIHEN) was used to facilitate the control of arc current. Pure iron wire with a diameter of 1.2 mm was used as the filler material, and the wire feed rate was manipulated by setting the wire on a single-axis slider. The shielding gas was pure argon, supplied at a rate of 25 L/min. The test jig was equipped with two symmetrically arranged tungsten cathodes (see Fig. 1(b)). The distance between the cathode tips, referred to as the 'inter-cathode distance,' was one of the variable parameters (see Fig. 2). Table 1 provides specific details related to the experimental equipment.

The definitions of other variable parameters are also presented in Fig. 2. The wire extension is the distance that the wire extends from the contact tip to the solid–liquid interface of the wire. The arc length was defined as the distance between the solid–liquid interface and the tip of the tungsten

L_{ex}	Wire extension
L_{arc}	Arc length
L_{CTWD}	Contact tip to work distance (CTWD)
D_{ic}	Inter-cathode distance

Fig. 2 Definitions of wire extension, arc length, contact tip to work distance, and inter-cathode distance

Fig. 1 Schematic diagram of experimental setup: **a** general view of MIG-based non-transferred arc system and **b** top view of test jig used to fix tungsten cathodes

Table 1 Specifications and details of experimental equipment

Element	Specification
Shielding gas	Pure Ar
Gas flow rate	25 L/min
Tungsten cathodes	W-2 wt.% La_2O_3
Cathode diameter	1.6 mm
Tip angle	30°
Wire diameter	1.2 mm
Wire material	Pure Fe

cathodes. In this study, the term 'contact tip to work distance (CTWD)' is used to refer to the sum of the wire extension and arc length, which is the distance from the contact tip to the tungsten cathodes. This deviates from the conventional definition of CTWD, which typically refers to the distance from the contact tip to the workpiece. This redefinition was necessitated by the unique configuration of our setup, which included the use of tungsten cathodes.
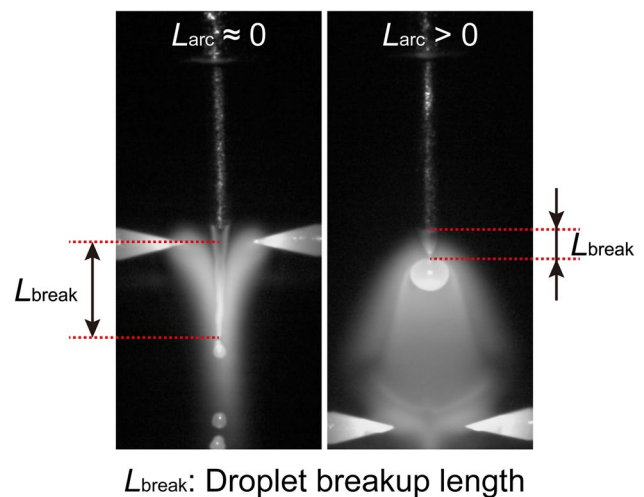
Our experiments were divided into three groups, A, B, and C, with each group focusing on a different variable parameter: arc length, inter-cathode distance, and wire extension, respectively (Table 2). For each group, inter-cathode distance, CTWD, arc current, and wire feed rate were directly controlled, which in turn indirectly affected the arc length and wire extension. Each set of experiments was repeated three times to ensure the reliability of the results. For Group C, it is important to note that changes in the CTWD also altered the nozzle standoff distance, which is the distance from the gas nozzle tip to the tungsten cathodes. This could potentially affect the shielding gas coverage, and thereby the arc properties and the metal transfer process. However, our experimental setup was designed in a way to minimize such influence by maintaining a consistent gas flow rate and an optimal nozzle standoff distance.

A high-speed camera (Memrecam HX-7, Nac Image Technology) captured the metal transfer process at 8000 fps, with a 45-W, 976-nm semiconductor laser providing lighting. The camera was positioned perpendicular to the cathode axis, allowing for simultaneous observation of metal transfer and arc geometry between the cathode gap, as shown in Fig. 1(b). The captured images were processed and analyzed to determine the metal transfer mode, metal transfer frequency, and droplet breakup length. Herein, we defined the droplet breakup length as the height of the liquid column between the solid–liquid interface (or the tungsten cathode tip) and the droplet detachment point, as shown in Fig. 3. Specifically, to determine the metal transfer frequency, we extracted frames capturing the occurrence of droplet breakup during the quasi-steady arcing time from all recorded images. Then, within these breakup frames, we counted each detached droplet and defined the metal transfer frequency as the number of droplets per second. For quantifying the droplet breakup length, each breakup frame was converted into binary images. This conversion facilitated the precise identification of the solid–liquid interface and the droplet detachment point, enabling accurate measurement of the droplet breakup length.

3 Results

In this study, we investigated the effects of varying arc length, inter-cathode distance, and wire extension on the metal transfer characteristics during the arc process. These parameters were independently controlled in three experimental groups (A, B, and C), each focusing on a specific aspect of the process.

L_{break}: Droplet breakup length

Fig. 3 Definition of droplet breakup length

Table 2 Experimental groups based on variable parameters

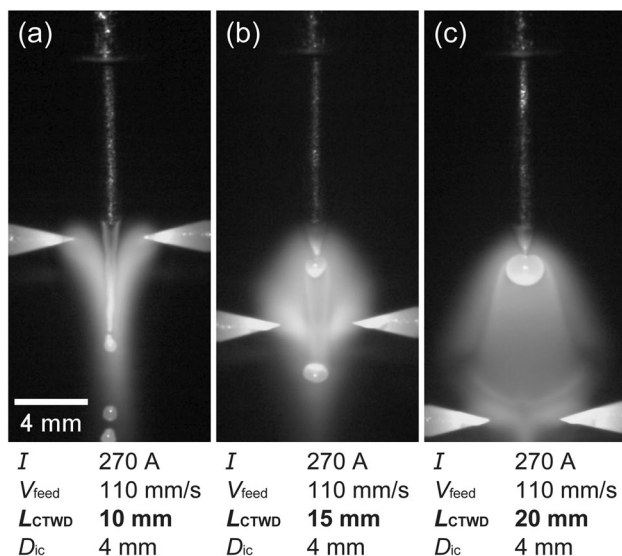| Group	Wire extension (mm)	Arc length (mm)	Inter-cathode distance (mm)	CTWD (mm)	Arc current (A)	Wire feed rate (mm/s)
A	Fixed	Varies	4	10, 15, 20	270	110
B	Fixed	Fixed	4, 8, 10	15	270	110
C	Varies	Fixed	4	10, 20, 30	210	90, 105, 120

For Group A, we altered the arc length by adjusting the CTWD, while maintaining a constant wire feed rate and thus keeping the wire extension consistent. For Group B, we manipulated the inter-cathode distance. For Group C, we varied wire extension by manipulating the wire feed rate and CTWD, keeping the arc length almost constant. Detailed results of these experiments, showing the relationship between these parameters and the metal transfer characteristics, will be discussed in the following sections.
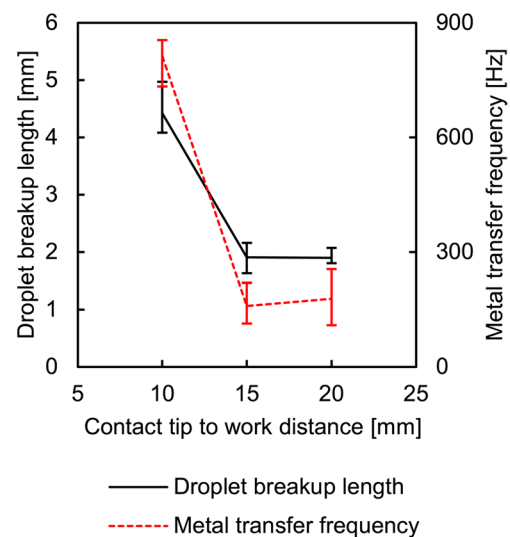
3.1 Group A: varying arc length

In Group A, the arc length was adjusted by varying the CTWD, while the inter-cathode distance, arc current, and wire feed rate were kept constant at 4 mm, 270 A, and 110 mm/s, respectively. Consequently, this maintained the wire extension at an approximate fixed value of 10 mm. Figure 4 presents high-speed images corresponding to arc lengths of 0, 5, and 10 mm.

For an arc length of 0 mm, we primarily observed streaming-spray transfer mode. As we increased the arc length to 5 mm, projected-spray transfer became the most common mode, although instances of globular transfer were still occasionally observed. A further increase in the arc length to 10 mm led to the exclusive dominance of the globular transfer mode. These observations underscore that an increase in arc length prompts a transition in metal transfer modes, with an increased propensity for globular and projected-spray transfer as arc length extends.

Figure 5 presents the variation in average droplet breakup length and metal transfer frequency with the arc length. At an arc length of 0 mm, the breakup length and

Fig. 5 Average droplet breakup length and metal transfer frequency as arc lengths increase in Group A

frequency had notably high values, recorded as 4.42 mm and 811.8 Hz, respectively. As the arc length increased to 5 mm or longer, they significantly decreased, with the breakup length being less than half and the transfer frequency one-fifth that of the 0-mm case. Our results indicate that whether the arc length was zero or longer had a significant impact on metal transfer characteristics.
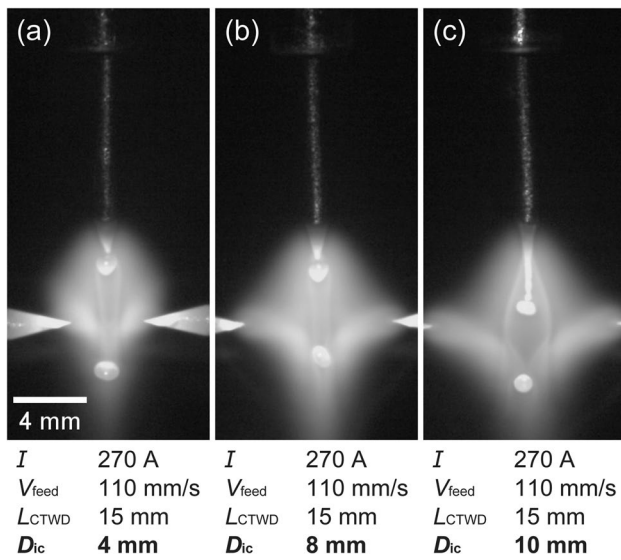
It should be also noted that the arc length values were obtained from high-speed images and exhibit a degree of temporal variation due to the dynamic nature of the arc process. In each condition, the arc length could fluctuate within a maximum range of 1 mm. This temporal variation introduces a degree of error in the specific arc length measurements. However, this variation is minor relative to the absolute value of the arc length, and the overall trends and conclusions drawn from this study remain indicative of the overall behavior of the arc process under varying conditions.

3.2 Group B: varying inter-cathode distance

In Group B, we focused our attention on the effects of varying the inter-cathode distance. We adjusted the inter-cathode distance while keeping the other parameters constant, with the CTWD at 15 mm, the arc current at 270 A, and the wire feed rate at 110 mm/s. Consequently, we were able to maintain a wire extension of roughly 10 mm and an arc length of approximately 5 mm.
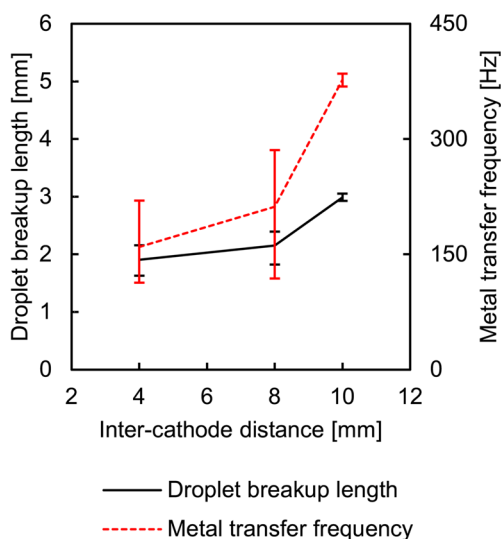
High-speed images corresponding to inter-cathode distances of 4, 8, and 10 mm are presented in Fig. 6. All three conditions observed both the projected- and streaming-spray transfer modes. The dominant metal transfer mode

I	270 A	I	270 A	I	270 A
V_{feed}	110 mm/s	V_{feed}	110 mm/s	V_{feed}	110 mm/s
L_{CTWD}	**10 mm**	L_{CTWD}	**15 mm**	L_{CTWD}	**20 mm**
D_{ic}	4 mm	D_{ic}	4 mm	D_{ic}	4 mm

Fig. 4 Metal transfer images for Group A with arc length of **a** 0, **b** 5, and **c** 10 mm

Fig. 6 Metal transfer images for Group B with inter-cathode distance of **a** 4, **b** 8, and **c** 10 mm

transitioned from projected- to streaming-spray transfer at 10 mm. One observable trend in the high-speed images was that with the increase in the inter-cathode distance, the droplet breakup length tended to lengthen: 1.91 mm at 4 mm, 2.16 mm at 8 mm, and 2.99 mm at 10 mm. Furthermore, even under the condition of streaming-spray transfer (inter-cathode distances of 10 mm), droplet detachment occurred relatively periodically. Figure 7 further illustrates the increase in average transfer frequency with the inter-cathode distance: 159.6 Hz at 4 mm, 211.8 Hz at 8 mm, and 377.4 Hz at 10 mm.
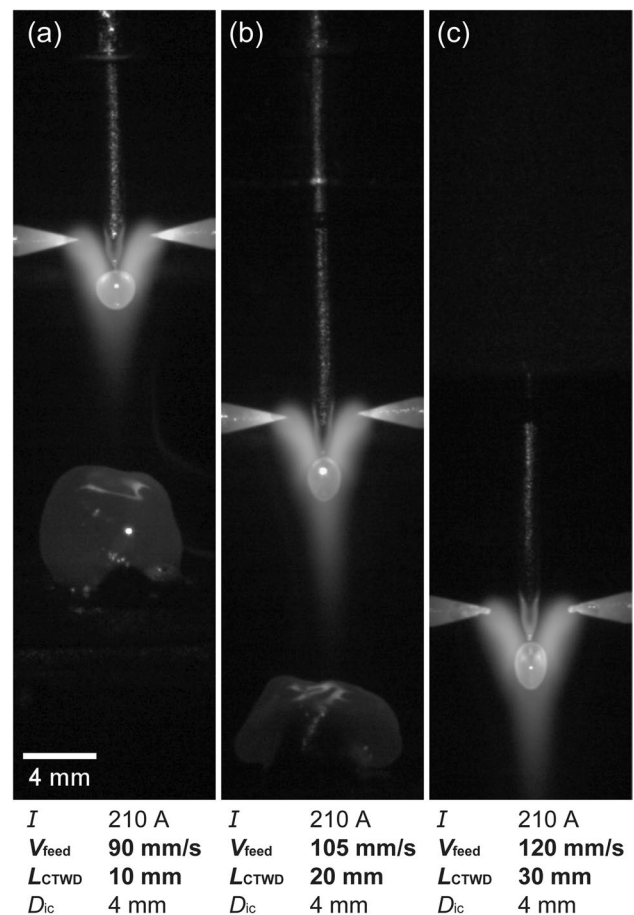

Fig. 7 Average droplet breakup length and metal transfer frequency as inter-cathode distances increase in Group B

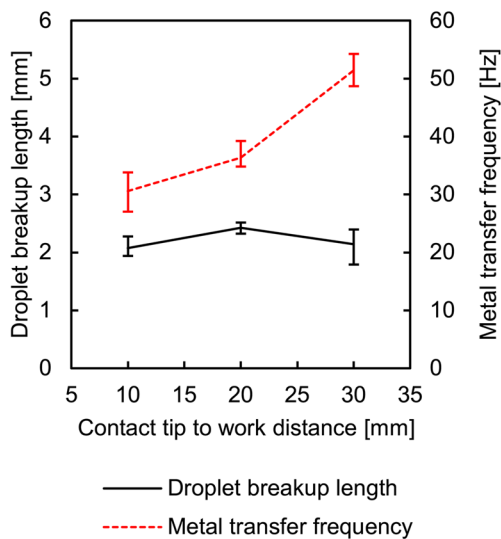## 3.3 Group C: varying wire extension

In Group C, the wire extension served as the variable of interest. To control it, we manipulated the CTWD and wire feed rate while maintaining the inter-cathode distance and arc current at consistent values of 4 mm and 210 A, respectively. Consequently, this strategy kept the arc length fixed at 0 mm. Figure 8 displays high-speed images corresponding to wire extensions of 10, 20, and 30 mm.

As seen in Fig. 8, all conditions exhibited a projected-spray transfer mode, irrespective of the wire extension. This implies that an increase in wire extension from 10 to 30 mm did not trigger a transition in the metal transfer mode. The results emphasize the isolated impact of wire extension under our specialized conditions of minimized arc length, a feature unavailable in conventional welding setups.

In support of our observations, Fig. 9 shows that the droplet breakup length stayed relatively constant, fluctuating around 2 mm. However, in terms of average transfer frequency, a trend of gradual increase with longer wire extension was observed. More specifically, the metal

Fig. 8 Metal transfer images for Group C with wire extension of **a** 10, **b** 20, and **c** 30 mm

Fig. 9 Average droplet breakup length and metal transfer frequency as wire extensions increase in Group C

transfer frequency rose from 30.6 Hz at a wire extension of 10 to 51.4 Hz at a wire extension of 30 mm. These results indicate that the metal transfer characteristics in this specific experimental configuration are not so sensitive to changes in wire extension.

4 Discussion

In our research, we meticulously manipulated three principal parameters—arc length, inter-cathode distance, and wire extension—to assess their effects on metal transfer characteristics. Each of these parameters was selected to control distinct driving forces in GMAW. Changes in arc length and inter-cathode distance were designed to modify the arc geometry or the current path, thus indirectly influencing the electromagnetic forces. Concurrently, wire

extension, inherently linked to the wire feed rate, was varied to observe its effect on the inertial forces in metal transfer.

4.1 Groups A and B: varying arc geometry

Molten droplets are subjected to the electromagnetic force induced by arc current. The path of the arc current, which expands from the molten droplet to the surrounding arc plasma, is believed to be closely related to the magnitude of the electromagnetic force. Furthermore, the current path is determined by the arc geometry, where the arc length and inter-cathode distance serve as evaluation parameters for this arc geometry. Specifically, the arc length includes a longitudinal aspect of the arc geometry, and the inter-cathode distance includes a radial aspect of the arc geometry.
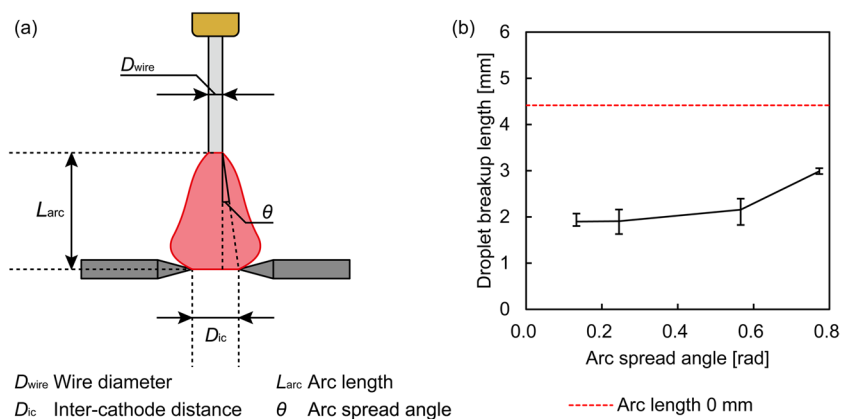
Based on our observations, when the arc length decreased, the droplet breakup length tended to increase. Especially, it was confirmed that the droplet breakup length significantly extended when adopting a unique condition where the arc length became approximately zero. On the other hand, it was demonstrated that an increase in inter-cathode distance also resulted in an increase in the droplet breakup length.

According to our experimental setup, the arc geometry can be simplified by a trapezoid connecting the wire tip to the tungsten cathode tips, as depicted in Fig. 10. In this trapezoid, the arc length corresponds to the height, the inter-cathode distance corresponds to the length of the bottom base, and the wire diameter corresponds to the length of the top base. This trapezoidal representation allows us to derive the 'arc spread angle,' which is the angle formed between the vertical height and the slanted sides of the trapezoid. The arc spread angle is defined by Eq. (1), and its evaluation results are shown in Fig. 10.

$$\theta = \tan^{-1}\frac{D_{ic}-D_{wire}}{2L_{arc}}, \# \tag{1}$$

where θ denotes the arc spread angle and D_{ic}, D_{wire}, and L_{arc} are the inter-cathode distance, wire diameter, and arc

Fig. 10 Longitudinal and radial evaluations of arc geometry: **a** definition of arc spread angle and **b** average droplet breakup length against arc spread angle in Groups A and B

length, respectively. From this definition, the decrease in arc length and the increase in inter-cathode distance result in an increase in arc spread angle. Figure 10 indicates that increasing the arc spread angle resulted in the elongation of molten droplets. It is crucial to mention, though, that our definition of the arc spread angle cannot apply when the arc length is zero. Consequently, in Fig. 10, the droplet breakup length for an arc length of 0 mm is presented for reference using a red dotted line.

A potential impact of the increasing arc spread angle on electromagnetic force is the decrease in current density inside the molten droplet. In general, the square of current density determines the magnitude of electromagnetic pressure. As the current density decreases, the electromagnetic pressure at the droplet tip reduces, potentially increasing the electromagnetic pressure gradient inside the molten droplet, as illustrated in Fig. 11. As a result, the molten droplets seemed to elongate more with larger arc spread angles. Ogino et al. have previously demonstrated through numerical calculations that an increased arc spread angle transitions the metal transfer mode from globular to streaming-spray transfer [8, 9]. Their findings are consistent with our analysis. Furthermore, a similar trend is observed in the occurrence of streaming-spray transfer mode in argon-rich gas-shielded welding where the arc plasma spreads easily. This contrasts with carbon dioxide welding where arc constriction is predominant.
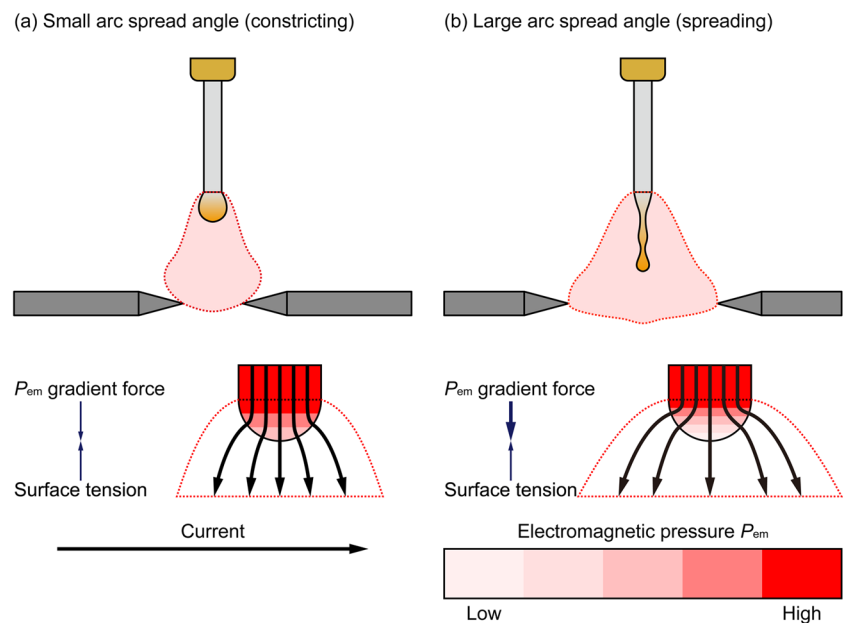
4.2 Group C: varying wire extension

Research in fluid dynamics, particularly studies on orifice dripping, provides an interesting context for considering the metal transfer dynamics in GMAW. In orifice dripping, faster outflow speeds have been found to affect the jet breakup behavior, due to increases in inertial force compared to surface tension [10, 11]. This raises the possibility that in GMAW, the wire feed rate could similarly impact metal transfer behaviors through inertial force. Herein, it is important to note that the exact relationship between wire feed rate and metal transfer characteristics remains unclear from a driving force perspective. As the wire feed rate and welding current are intertwined in conventional GMAW setups, few studies have focused on the effect of wire feed rate.

It is well established that the wire feed rate is governed by Joule heating in the wire extension and arc heating at the wire tip, both of which can be modulated by the welding current [1]. In our unique setup, by maintaining a constant arc current at 210 A and holding the arc length at 0 mm, the wire feed rate exhibits an almost linear relationship with the wire extension length. This configuration allows for a precise evaluation of the direct impact of wire feed rate on metal transfer dynamics from a driving force perspective.

In our experiments, as the wire extension increased to 10, 20, and 30 mm, the wire feed rate correspondingly increased to 90, 105, and 120 mm/s. Notably, even with the rise in the

Fig. 11 Mechanism of arc spread angle affecting metal transfer: **a** small and **b** large arc spread angles

wire feed rate, neither the metal transfer mode nor the droplet breakup length exhibited any perceptible alterations. The only observed variation was in the metal transfer frequency, which exhibited an increase. Indeed, the convection induced by wire feeding generates inertial force. However, our observations indicate that the inertial force could be insufficient to overcome surface tension and elongate the molten droplet, especially in the globular transfer mode where surface tension is predominant. While the droplet breakup length remained consistent, the increase in wire feed rate boosted the mass flow rate, leading to faster formation of similarly sized droplets. This likely accounts for the observed rise in metal transfer frequency.

On the other hand, Lesnewich reported contrasting findings that an increase in wire extension leads to a reduction in the critical current, above which the metal transfer mode transitions from globular to axial-spray transfer [12]. Given an apparent inconsistency between our results and those of Lesnewich, the following considerations should be made carefully: our evaluation parameters and the targeted metal transfer transition differed from Lesnewich's. He focused on droplet size to assess the transition between globular and axial-spray transfer modes, whereas our study delved into droplet breakup length, targeting the transition from projected- to streaming-spray transfer. Hence, Lesnewich's findings that faster wire feed rates reduce droplet size at lower welding currents do not rule out our results that droplet elongation is unaffected by wire feed rate.

It is worth noting a limitation in our study. The magnitude of inertial forces acts proportional to the square of the characteristic flow velocity. If the wire feed rate increases significantly, as with smaller diameter wires, it remains conceivable that inertial forces could serve as a secondary factor that interacts with and enhances the effects of the electromagnetic force on metal transfer.

5 Conclusion

We have developed a MIG-based non-transferred arc device that arranges tungsten cathodes symmetrically, enabling the arbitrary control of arc geometry and wire feed rate independent of arc current. Using this device, we meticulously examined the metal transfer characteristics in response to variations in three critical process parameters: arc length, inter-cathode distance, and wire extension. Our primary findings are summarized as follows:

(1) Both arc length and inter-cathode distance were effective for two-dimensional control of the arc geometry. In particular, either a shorter arc length or a longer inter-cathode distance widened the arc current path, enhancing the electromagnetic force on the molten droplets.

(2) The impacts of arc length and inter-cathode distance could be consistently evaluated using the arc spread angle θ. As a result, it was confirmed that an increase in the arc spread angle contributes significantly to droplet elongation.

(3) An increase in wire extension led to a rise in wire feed rate, subsequently causing an increase in inertial force. However, we did not identify this increase in inertial force to induce any changes in metal transfer modes. Under extreme experimental conditions, such as when the wire extension is set beyond 30 mm and the wire feed rate is accelerated, there remains a possibility that the inertial force might influence the transfer mode.

Based on these findings, we clarified the relationship between driving forces and process parameters, offering a more precise guideline for controlling metal transfer in GMAW. However, in actual welding scenarios, the influence of the molten pool oscillation on the arc geometry becomes more intricate. As a future challenge, there is anticipation for the establishment of an electromagnetic force evaluation model considering three-dimensional arc geometries and its potential application to welding current control techniques.

Declarations

Conflict of interest The authors declare no competing interests.

References

1. Hirata Y (1995) Physics of welding (III)—melting rate and temperature distribution of electrode wire. Weld Int 9:348–351. https://doi.org/10.1080/09507119509548811
2. Scotti A, Vladimir P, Lucas W (2012) A scientific application oriented classification for metal transfer modes in GMA welding. J Mater Process Technol 212:1406–1413. https://doi.org/10.1016/j.jmatprotec.2012.01.021
3. Ogino Y, Hirata Y (2015) Numerical simulation of metal transfer in argon gas-shielded GMAW. Weld World 59:465–473. https://doi.org/10.1007/s40194-015-0221-8

4. Lancaster JF (1986) The physics of welding, 2nd edn. Pergamon Press

5. Ando K, Nishiguchi K, Fukuda K (1967) Temperature characteristics of the droplet detaching from the wire tip in MIG welding—effect of the Joule's preheating. Q J Jpn Weld Soc 36:1117–1124. https://doi.org/10.2207/qjjws1943.36.1117

6. Wang J, Wu D, Liao P et al (2013) Metal transfer and arc behaviour of novel consumable and non-consumable electrode indirect arc droplet welding. Sci Technol Weld Join 18:261–270. https://doi.org/10.1179/1362171812Y.0000000103

7. Zhu Y, Wang Z, Liu R, Liu L (2022) Study on arc behavior and droplet transfer in twin-electrode TIG-MIG indirect arc welding. Int J Adv Manuf Technol 120:6821–6831. https://doi.org/10.1007/s00170-022-09131-1

8. Ogino Y, Hirata Y, Kihana S, Nitta N (2018) Numerical simulation of free-flight transfer by a 3D metal transfer model. Q J Jpn Weld Soc 36:94–103. https://doi.org/10.2207/qjjws.36.94

9. Ogino Y, Hirata Y, Asai S (2020) Discussion of the effect of shielding gas and conductivity of vapor core on metal transfer phenomena in gas metal arc welding by numerical simulation. Plasma Chem Plasma Process 40:1109–1126. https://doi.org/10.1007/s11090-020-10102-1

10. Leib SJ, Goldstein ME (1986) The generation of capillary instabilities on a liquid jet. J Fluid Mech 168:479–500. https://doi.org/10.1017/S0022112086000472

11. Eggers J (1997) Nonlinear dynamics and breakup of free-surface flows. Rev Mod Phys 69:865–929. https://doi.org/10.1103/RevModPhys.69.865

12. Lesnewich A (1958) Control of melting rate and metal transfer in gas-shielded metal-arc welding—part II—control of electrode metal transfer. Weld J 37:418–425